PNAS RESEARCH ARTICLE | APPLIED PHYSICAL SCIENCES EVOLUTION

Evolutionary features in a minimal physical system: Diversity, selection, growth, inheritance, and adaptation

Guy Bunin[a,1,2] and Olivier Rivoire[b,1,2]

Edited by Stanislas Leibler, The Rockefeller University, New York, NY; received December 10, 2024; accepted June 20, 2025

We present a simple physical model that recapitulates several features of biological evolution, while being based only on thermally driven attachment and detachment of elementary building blocks. Through its dynamics, this model samples a large and diverse array of nonequilibrium steady states, both within and between independent trajectories. These dynamics exhibit directionality with a quantity that increases in time, selection, and preferential spatial expansion of particular states, as well as inheritance in the form of correlated compositions between successive states, and environment-dependent adaptation. The model challenges common conceptions regarding the requirements for life-like properties: It does not involve separate mechanisms for metabolism, replication, and compartmentalization; stores and transmits digital information without template replication or assembly of large molecules; exhibits selection both without and with reproduction; and undergoes growth without autocatalysis. As the model is based on generic physical principles, it is amenable to various experimental implementations.

evolution | origin of life | reproduction

Significance

Understanding how a physical or chemical system can acquire characteristics of biological evolution is fundamental for elucidating the origin of life and for engineering systems that mimic biological processes. We propose a simple approach to generate evolutionary-like processes. Unlike most previous approaches, it does not rely on autocatalysis. Instead, we design a system that can exist in a large number of out-of-equilibrium states, with growth, replication, selection, and adaptation emerging as properties of its dynamics. Based on fundamental physical principles, this model can be implemented experimentally in the fields of systems chemistry or soft-matter physics.

Life is understood as both the product and the engine of evolutionary processes. In extant life forms, reproduction of individuals with heritable variation, which is required for Darwinian evolution, involves complex chemical and physical processes orchestrated by intricate biomolecules that are, moreover, themselves the product of evolution. The intricacy of these processes poses a significant challenge for conceptualizing life and understanding how it originated. This challenge motivates the development of simple physical models capable of mimicking biological evolution as an approach to elucidate the minimal requirements for life-like features.

The focus of many efforts has been the design of simple computational (1) or physical systems capable of reproduction. The latter range in scale from centimeters (2) to microns (3) and nanometers (4, 5). The designs typically require ingenious mechanisms and rely on external drives such as temperature cycling. Their common underlying principle is autocatalysis, where one element promotes the formation of other elements of the same type (6) or, more generally, where several elements collectively promote their reproduction (7).

In any case, reproduction alone is not sufficient for Darwinian evolution: Significant diversity must also be generated and inherited. Assemblies that reproduce by template replication, either in the form of heteropolymers (8), supramolecular polymers (9) or growing crystals (5, 10), are often taken as carriers of diversity. An alternative is to take as carriers of diversity compositional states, defined by the relative concentration of a set of chemical species (11). In this context, it has been proposed that evolution may operate through transitions between autocatalytic "cores," each supported by a different subset of molecules (12). However, no experimentally feasible proposal has been made. Besides, it has been argued that additional processes, such as low-rate background reactions or the presence of compartments, may be necessary for evolution to occur by this process (13). In light of these considerations, developing simple physical models capable of mimicking biological evolution remains a central and open challenge.

Here, we propose a theoretical but physical and generic model that features directionality, diversity, selection, growth, inheritance, and adaptation. It does not include autocatalysis, compartments, or assemblies into large molecules, demonstrating that they are not necessary for generating these evolutionary features.

1. Model

We provide three levels of description for our model: a physical description that defines the fundamental components and their interactions, prescribing how these components

Author affiliations: [a]Department of Physics, Technion-Israel Institute of Technology, Haifa 32000, Israel; and [b]Gulliver, CNRS, École Supérieure de Physique et Chimie Industrielles, Université Paris Sciences & Lettres, Paris 75005, France

Author contributions: G.B. and O.R. designed research; performed research; contributed new reagents/analytic tools; analyzed data; and wrote the paper.

The authors declare no competing interest.

This article is a PNAS Direct Submission.

[1]G.B. and O.R. contributed equally to this work.

[2]To whom correspondence may be addressed. Email: buning@technion.ac.il or olivier.rivoire@espci.fr.

This article contains supporting information online at https://www.pnas.org/lookup/suppl/doi:10.1073/pnas.2425753122/-/DCSupplemental.

Published July 30, 2025.

bind and unbind due to thermal fluctuations; a detailed chemical description that lists the elementary reactions between the components; and a coarse-grained chemical description that retains only the key dynamical variables, from which the results presented in the figures are generated.

The three levels of description serve different purposes. The last, coarse-grained level is employed in numerical simulations to generate the results that we present. It is derived, under certain specified conditions, from the description of all elementary chemical reactions and their respective rates. This detailed chemical description, which can also be used to study thermodynamics, often serves as a starting point in models related to the origin of life. Here, we derive it from a more fundamental physical description. This approach ensures physical consistency, provides guidance for experimental implementation, and allows us to account for critical physical and geometric constraints that are not considered in chemical models based solely on thermodynamics—constraints often associated with "molecular and functional complexity."

For example, these constraints explain why experiments with nonenzymatic autocatalysis often exhibit nonexponential growth (4), as one manifestation of these constraints is product inhibition (14). They also underlie the difficulty of evolving replicases large enough to allow faithful replication (15), which led to the proposal of a threshold known as the error catastrophe (16), again unexplained by thermodynamics. More generally, the purported need for large molecules to support evolutionary processes motivates many proposals that use molecular complexity as a biosignature (17). By defining our model at the physical level, we make explicit what we mean by a minimal and physical model, namely one based only on rigid objects that does not require or assume any assembly or any enzyme-like mechanism.

1.1. Physics and Chemistry. Inspired by a model in theoretical ecology showing how networks of inhibitory interactions lead to many stable states, and directional dynamics over long time scales with regimes of spatial expansion (18), we define a chemical system with a similar network of inhibitory interactions between constituents. The stable states of the chemical system are defined by the concentrations of N reactants A_i, $i = 1..N$. The production of each A_i is promoted by a catalyst C_i, which can be inhibited by the presence of certain other A_j. This can lead to multistability, where certain reactants are "active," i.e. found at high levels, and prevent others from being catalyzed at significant rates. This multistability generally requires a nonlinear dependence of the inhibition of C_i on the concentration of the inhibiting A_j (19). One mechanism often encountered in biological systems is cooperativity, where inhibition involves two or more A_i that interact nonadditively. Another mechanism is inhibitor ultrasensitivity (20), which requires only the presence of another molecule B_i that strongly binds to A_i. We adopt this simpler mechanism where the nonlinearity arises from the necessity for A_i to first saturate B_i before effectively inhibiting C_j.

The reaction that produces A_i could be of various types. To emphasize that neither large molecules nor assembly are important, we consider A_i to result from the dissociation of a dimer A_iA_i' (Fig. 1*A*). B_i is defined as another monomer that forms a dimer A_iB_i when it interacts with A_i. This interaction is through the interface by which A_i interacts with both A_i' and C_j, so that B_i and C_j interact with A_i but not with A_iA_i' (Fig. 1*A* and *SI Appendix*, section A). The catalyst C_i accelerates the cleavage reaction $A_iA_i' \rightarrow A_i + A_i'$ without being consumed. In biology, most catalysis is mediated by enzymes, which are large

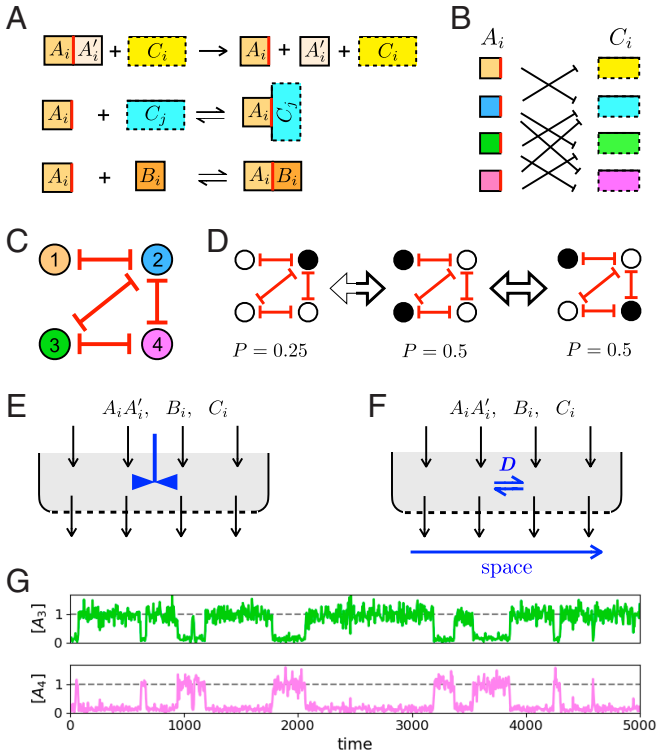

Fig. 1. (*A*) We consider N reactions ($i = 1..N$) involving the dissociation of dimers A_iA_i' into monomers A_i and A_i', catalyzed by C_i. The product A_i can bind to and inhibit the catalyst C_j of another reaction j. In addition, A_i can bind to B_i to form a dimer A_iB_i. (*B*) Inhibition is reciprocal: If A_i inhibits C_j, then A_j inhibits C_i. (*C*) The network of reciprocal inhibition forms a graph where nodes represent reactions i, and edges reciprocal inhibition. (*D*) Representation of the 3 stable states associated with the graph in (*C*). By default, a node is active unless repressed by an active neighboring node. In a stable state, a node is active (in black) if and only if all the nodes to which it is connected are inactive (in white). The productivity P of a state is the fraction of active nodes. Transitions between states exhibit directionality, predominantly occurring from low to high productivity states. (*E*) The reactions take place in an open reactor where A_iA_i', B_i, and C_i are continuously injected and where all species are continuously diluted out. When the system is well mixed, the reactants are homogeneously distributed throughout the reactor. (*F*) Injection and dilution are homogeneous in space, but heterogeneities can arise from stochastic fluctuations and the limited diffusion of all species along a one-dimensional direction. (*G*) Example trajectory for the concentrations $[A_i]$ associated with nodes $i = 3$ and 4 of the graph in (*C*) in the well-mixed case, showing stochastic switches between the two states with highest productivity $P = 0.5$ ($[A_1] \simeq 1$ and $[A_2] \simeq 0$ remain roughly constant; see *SI Appendix*, Fig. S1).

molecules. To implement an elementary form of nonenzymatic catalysis, we define C_i as a rigid body with two interacting sites for binding to A_i and A_i', which achieves catalysis provided that the distance between these two interacting sites and their affinity are in appropriate ranges (21, 22).

An essential aspect of the model is the topology of the network of inhibitory interactions. Each A_i does not inhibit every C_j but only a small number (small compared to N), and the inhibition is reciprocal: If A_i inhibits C_j, then A_j also inhibits C_i (Fig. 1*B*). This choice is motivated by general results in statistical mechanics and theoretical ecology showing that such sparse reciprocal interactions allow one to obtain a large number of stable states (18, 23, 24). The structure of the reciprocal inhibitory interactions is summarized in an undirected graph, where each node represents a reaction i (Fig. 1*C*). Below, we take a random-regular graph with connectivity $c = 3$, that is, randomly chosen from graphs where each node is connected to exactly three other nodes.

1.2. Effective Reaction Kinetics. We study the reactions in the setting of an open system where the substrate A_iA_i' for the production of A_i, the binders B_i, and the catalysts C_i are supplied externally at a constant flux, and where all chemical species are continuously diluted out at a constant rate. If the system is well mixed, this corresponds to a chemostat setup (Fig. 1*E*). However, to obtain reproduction in our model, space is essential, and we therefore consider that each chemical species can diffuse in space with a diffusion constant that we take to be the same for all species (Fig. 1*F*). The supplied chemicals are delivered uniformly throughout space. For simplicity, we assume a one-dimensional space with periodic boundary conditions. Finally, the discreteness of the molecules induces stochasticity, also known as demographic noise in the context of evolutionary dynamics.

Such a system is described mathematically by a set of coupled reaction–diffusion Langevin equations (*SI Appendix*, section D). To simplify the presentation and analysis, we consider a limit where time-separation leads the dynamics to be effectively described by a set of only N equations. In this limit, the inhibition of C_j by A_i occurs on a faster timescale than the catalysis of A_i by C_i, and the binding of B_i to A_i on an even faster timescale (*SI Appendix*, section B). A large well-mixed system is then simply described by

$$\partial_t[A_i] = \frac{\Lambda_i}{1+\Gamma\sum_{j\sim i}\max(0,[A_j]-[B_j])} - \delta[A_i], \qquad [1]$$

where $[A_i]$ and $[B_i]$ represent the concentration of the elements A_i and B_i, including those in the form of a dimer A_iB_i, but excluding the dimers A_iA_i'. In this limit, $[B_i]$ is constant and can be treated as a model parameter. The first term of the equation represents inhibited catalysis, where the sum in the denominator is over all the A_j that can potentially inhibit C_i, and the second term represents dilution at a rate δ. We first consider Λ_i to be the same for all i, which corresponds to a uniform supply of each substrates A_iA_i' and an equal catalytic efficiency of each catalyst C_i. Besides the graph of inhibitory interaction defining the relationships $i \sim j$, the equation has the following independent parameters: the inhibitory strength Γ, concentration $[B_i]$ which we take to be independent of i, corresponding to a uniform supply of all B_i, and the Λ_is (the dilution rate δ can always be absorbed into a redefinition of the time unit). This equation is generalized to include diffusion and demographic noise to describe the stochastic dynamics for the local concentration $[A_i](x,t)$ of molecules A_i at each spatial location x and time t (*SI Appendix*, section D). Diffusion is quantified by a diffusion constant D, and demographic noise by a parameter ω that scales with the inverse of the square root of the volume (*SI Appendix*, section C). We simulate these equations with a standard Euler–Maruyama algorithm, adding only a constraint to force $[A_i](x,t)$ to be nonnegative (*SI Appendix*, section F).

Unless otherwise stated, we fix the following parameters: $N = 50$, $\Lambda_i = 1$, $\Gamma = 10$, $\delta = 1$, $[B_i] = 0.25$, and $\omega = 0.1$. We discretize space in $M = 10$ or $M = 100$ cells of unit length, while keeping a constant diffusion constant $D = 1$. To simulate a corresponding well-mixed system, we divide ω by $\sqrt{M}$ and then set $M = 1$. The dynamics being stochastic whenever $\omega > 0$, different realization of the dynamics are obtained when starting from the same initial condition, which by default we take to be $[A_i](x, t = 0) = 0$ for all i and x.

2. Results

Simulations of the spatiotemporal dynamics described above show that variables spend most of the time fluctuating around two values, with abrupt switches between them: A_i is either "active," $[A_i] = \Lambda_i/\delta$, or "inactive," $[A_i] \simeq 0$ (Fig. 1*G*). These dynamics can be understood as fluctuations around stable states of the deterministic dynamics without demographic noise. Stable states are configurations of active and inactive A_i, where A_i is active if and only if all the A_j to which it is connected by inhibitory interactions are inactive (Fig. 1*D*). In graph theory, these states are known as the maximal independent sets of the inhibition graph. Enumerating them in a well-known combinatorial problem (25). Noise-driven jumps between the basins of different stable states involve switches between active and inactive values for a number of variables. The distribution of concentrations is therefore essentially bimodal (*SI Appendix*, Fig. S4*A*), although the concentrations may take intermediate values at the spatial boundaries separating two stable states.

An illustration of one realization of the process is shown in Fig. 2*A*. In this representation, borrowed from analytical chemistry (26), different colors represent different chemical compositions, with similar colors indicating similar compositions (*SI Appendix*, section F). At each space and time point, we identify the nearest stable state (*SI Appendix*, section F), which is a steady state for the deterministic dynamics without demographic noise. This nearest stable state essentially amounts to considering A_i as active or inactive depending on whether it is closer to 0 or to Λ_i/δ (*SI Appendix*, Fig. S4).

2.1. Extended Directional Evolution and Reproduction. We reproduce an observation first made in the context of an analogous Lotka–Volterra system with sparse inhibitory interactions (18): Changes occur on timescales that far exceed any microscopic timescale ($T = 10^5$ in Fig. 2 while all parameters in Eq. **1** are of order 1; see also *SI Appendix*, Figs. S2 and S3 for other sample trajectories with the same or different inhibitory

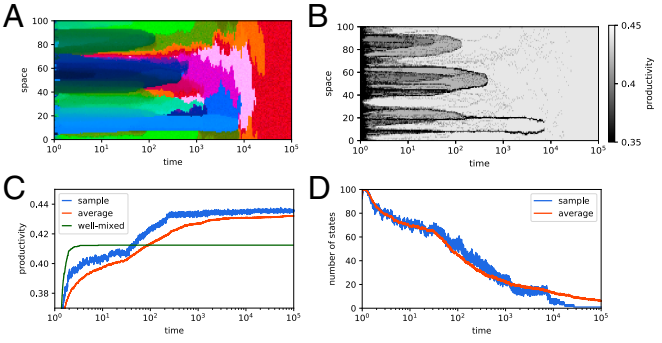

Fig. 2. (*A*) A representation of one trajectory in space and time using a low-dimensional projection of the relative concentrations $[A_i]$ to visualize different compositions by different colors (*SI Appendix*, section F). Here, the inhibition graph is a random regular graph with $N = 50$ nodes and connectivity $c = 3$. Space is divided in $M = 100$ cells and time is represented in log-scale (see *SI Appendix*, Fig. S2 for other sample trajectories from the same inhibitory graph and *SI Appendix*, Fig. S3 for sample trajectories from other graphs). (*B*) For the same trajectory, productivity, i.e, fraction of active A_i. (*C*) Mean productivity across space. For comparison, average over 20 different trajectories obtained with exactly the same parameters, and the result for a corresponding well-mixed system. The sample trajectory reaches the maximum productivity ($P = 22/50 = 0.44$) for the chosen inhibitory graph. (*D*) Evolution of the number of different stable states. The average value shows that while the sample trajectory ends up in a single state, this is not always the case (*SI Appendix*, Fig. S2).

graphs). Unlike the Lotka–Volterra system, however, our model does not have a Lyapunov function. Nevertheless, these changes are directional: The system evolves toward states of increasing "productivity," where productivity of a state is the fraction of active variables A_i in this state (Fig. 2 *B* and *C*). Configurations sampled through the dynamics are not strictly stable states but the productivity of a configuration can be defined by considering the nearest stable state to that configuration. A directional evolution toward higher productivity is also obtained in well-mixed systems (Fig. 2*C* and *SI Appendix*, Fig. S5), in which case it can be understood formally. For well-mixed systems with strong inhibition (large Γ) and low noise (small ω), transitions between states are indeed entirely driven by fluctuations that reduce the concentrations of active variables, which then allows previously inactive neighboring variables to become active. The transition from a high-productivity state to a low-productivity state requires more of these fluctuations and is therefore less probable than the reverse transition (*SI Appendix*, section E). This asymmetry in transition probabilities results in directional dynamics that favor progression toward higher productivity states over time.

When mixing is not instantaneous, allowing for variation in space, the dynamics is more complex and this increase in productivity is accompanied by a spatial expansion of some states at the expense of others, which is a form of reproduction. This is evidenced by a decrease in the number of different states as a function of time (Fig. 2*D*).

2.2. Diversity and Selection. When starting multiple replicate trajectories from the same all-zero initial condition (Fig. 3*A*), a large number of different stable states are attained in a finite time (Fig. 3*B*). Measured by the Shannon diversity, the number of states is in the thousands (in this instance, around 3,000 states; *SI Appendix*, section F). Moreover, these states are very different from each other (Fig. 3*C*). However, this diversity is far less than the total number of stable states, which for the particular inhibitory graph used in Figs. 2 and 3, is $\mathcal{N} \simeq 4.8\ 10^5$. More generally, for random-regular graphs of connectivity $c = 3$, the number of stable states scales exponentially with the number N of nodes, as $\mathcal{N} \sim e^{Ns}$ with $s \simeq 0.26$ (*SI Appendix*, Fig. S7), and similarly for other random sparsely connected graph ensembles (24).

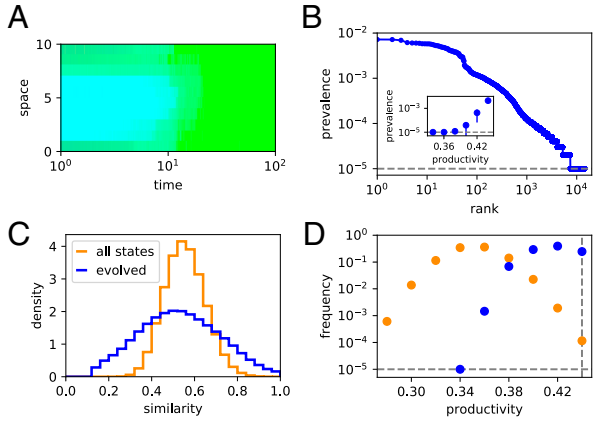

Fig. 3. (*A*) Illustration of the evolution of a system of size $M = 10$ over a time $T = 10^2$, starting from all $[A_i] = 0$. (*B*) When this evolution is repeated 10^5 times, some final states are reached more often than others: The most common are found in nearly 1% of the samples (prevalence $\sim 10^{-2}$) while the least common are found only once (prevalence 10^{-5}). *Inset*: Mean prevalence of states with given productivity, with error-bars indicating the SD of the distribution of prevalences. (*C*) Distribution of pairwise similarities between states, measured by the fraction of active or inactive A_i that two states share (in blue). For comparison, distribution of similarities between all stable states (in orange). (*D*) Distribution of productivity in evolved states (in blue) versus all stable states (in orange). The horizontal dashed line at frequency 10^{-5} marks the sampling limit given the 10^5 sample trajectories while the vertical dashed line marks the maximum productivity for this system.

As further evidence that selection is taking place, the subset of states that are reached most often are those with the highest productivity (Fig. 3*D*), which is consistent with the overall growth of productivity (Fig. 2*C*). Productivity is thus analogous to fitness: Current states with the highest productivity contribute more to future states. This is seen in the dynamics at intermediate and late times, $t \gtrsim 10$, where states of higher productivity are more likely to expand in space, leading to an increase in the average fitness (Fig. 2*A*). This analogy with fitness is further supported by the analysis of competitions below. Note, however, that productivity increases even in well-mixed systems in which reproduction by spatial expansion cannot occur (*SI Appendix*, Fig. S5), which represents a form of selection even in the absence of reproduction.

2.3. Heredity and Competition. In well-mixed conditions, successive states become increasingly similar over time, with the rate of change between states gradually decreasing. This trend can be interpreted as an evolution toward more accurate inheritance (*SI Appendix*, Fig. S5). Similar features are observed in systems with limited diffusion, as demonstrated by temporal correlation functions (*SI Appendix*, Fig. S6). Additionally, in systems with limited diffusion, certain states expand at the expense of others, exhibiting a form of reproduction that also involves inheritance. This spatial inheritance, which is a priori distinct from the increasing correlation in time, is quantified through spatial correlation functions (*SI Appendix*, Fig. S6).

To push this idea further, we consider competitions between two evolved states that are obtained by the dynamics of the previous subsection. The competition consists of initializing a system with these two states, each occupying half of the one-dimensional state space, and recording the state reached after a finite time (Fig. 4*A*). This usually results in a state that is different from either of the two competing states, but still much closer to one of them than to any other evolved state (Fig. 4*B*). When the two competing states have different productivity, this closest state is almost always the competing state with greater productivity (Fig. 4*C*), a result consistent with viewing productivity as a form of fitness.

The concepts of heredity and productivity are distinct: Heredity refers to persistent temporal correlations, while productivity refers to the number of active nodes. In our model, however, they increase concomitantly. In the well-mixed setting, at the low-noise limit (*SI Appendix*, section E), our model maps to a mean-field glass model (23), and this coupling reflects the well-known phenomenon of aging, where temporal correlations increase while energy decreases (27). Under limited diffusion, these effects are additionally coupled to spatial expansion (growth) and behavior under competition, features not typically associated with glassy systems.

2.4. Environments and Adaptation. In evolutionary biology, adaptation is contingent on the particular environment in which organisms evolve. Here, the environment comprises the substrates A_iA_i' that are injected. We have so far assumed that all substrates are injected at the same rate, but different environments can be defined by assuming that they are injected at different rates, which corresponds to taking Λ_i to depend on i in Eq. **1**.

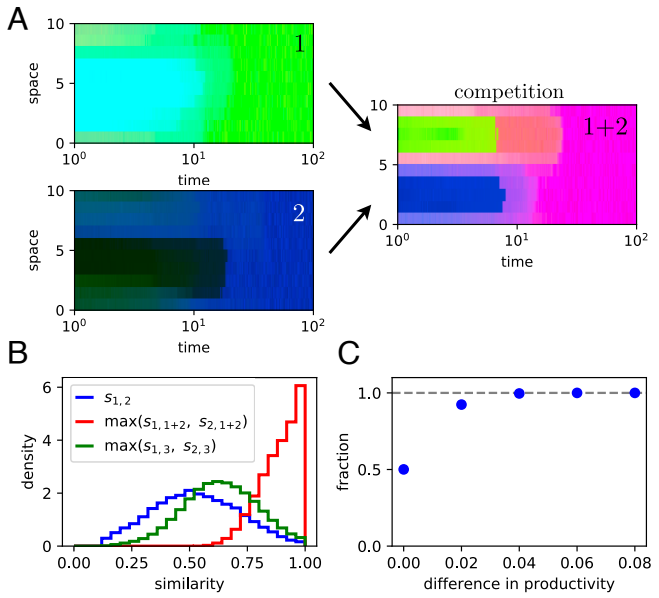

Fig. 4. (*A*) Two compositions obtained after evolution from the all-zero state (Fig. 3*A*) are competed against each other by juxtaposing them in space. (*B*) Distribution of pairwise similarities between the state resulting from the competition (1+2) and the closest of the two competing states (1 or 2). For comparison, we also show the closest similarity of another independently evolved state 3 to either 1 or 2, and the similarity between 1 and 2. (*C*) Fraction of times that the final state is more similar to the state with the higher productivity of the two initial competing states, as a function of the productivity difference between the two initial competing states.

If we take two states resulting from an evolution in two different environments and compete them in one of the two environments, we observe that the resulting state is most similar to the state that evolved in the same environment, consistent with the notion that this state is adapted to its environment (Fig. 5). We also note that in a well-mixed system, the expression for the productivity generalizes to provide an environment-dependent notion of fitness (*SI Appendix*, section E).

3. Discussion and Conclusion

While nearly every specific feature of living systems has a counterpart in one or more nonliving systems, understanding what is required for a physical system to exhibit the full range of features observed in living systems remains an open question. Here, we focus on a subset of evolutionary features: directionality, diversity, selection, growth, inheritance, and adaptation. In Darwinian evolution, diversity, differential reproduction, and inheritance form the foundations from which adaptation emerges through natural selection (28). Our model follows a different logic. Selection is present even in the well-mixed case, without spatial growth (*SI Appendix*, Fig. S5). Spatial variation, when mixing is not instantaneous, introduces a new resource—that is, space—over which competition can occur. This spatial resource transforms selection into a more Darwinian process in which more productive states grow at the expense of less productive ones (Fig. 2). This only begins after some time, consistent with the view that other forms of evolutionary adaptation, which do not require reproduction for selection and adaptation, may precede Darwinian evolution (29–31). Our model also does not consider metabolism, replication, and compartmentalization as separate processes that would need to be integrated (32). Instead, the same network of inhibitory reactions keeps the system in a state of disequilibrium, supports hereditary information, and induces spatial boundaries.

The essence of our model is an open dynamical system with a large number of stable steady states between which transitions occur stochastically, and which may expand in space. The analogy comparing states to biological species and state transitions to mutations in this context is not new and has been articulated particularly by Decker, who called such systems bioids (33). More generally, our model belongs to the broader class of models where the units of selection are relative molecular concentrations rather than specific (autocatalytic) molecules. Another model in this class is the GARD (Graded Autocatalysis Replication Domain) model, which describes autocatalytic growth of amphiphile assemblies (11).

Our model differs from these and previous models with compositional states in several ways. 1) It is based on simple rigid elements that attach and detach and does not require the presence or assembly of any large molecule. 2) It exhibits temporal directionality, with an emerging notion of "fitness" that predicts the outcome of competitions between states. 3) It exhibits "unlimited inheritance," i.e., the capacity to be in a number of states much larger than the number of states that it samples at any given time (34). 4) It does not involve autocatalysis.

The notion of autocatalysis is central to almost all previous models displaying evolutionary features, including those not based on compositional states. Autocatalysis is even often taken as synonymous with reproduction for a chemical system (35), with a distinction made between direct autocatalysis, where a molecule catalyzes its own formation, and reflexive (auto)catalysis, where a network of reactions is involved (36). Several proposals have been made to formalize autocatalysis and allow a nontautological association with growth and reproduction. Most of these formalizations focus primarily on necessary stoichiometric conditions (7, 12), i.e., conditions that a network of reactions must satisfy independently of kinetic rates or initial conditions. Our model does not satisfy these stoichiometric conditions. The feedback mechanism leading to multistability is based on inhibition rather than autocatalysis, and reproduction is observed only when spatial diffusion is considered: A well-mixed system that is defined by the same reactions shows mutations but neither growth nor reproduction. Unlike models based on stoichiometric autocatalysis, different states of our system are underlined by

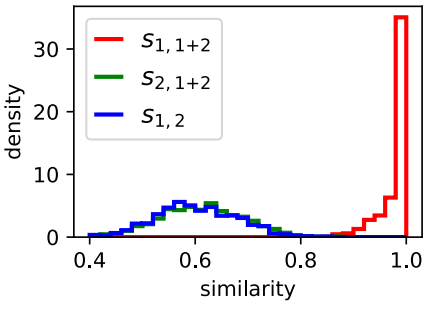

Fig. 5. An environment is defined by the influx rates of the substrates $A_iA'_i$ from which the A_i originate (Fig. 1*A*). Formally, it is specified by a N-dimensional vector with components Λ_i (Eq. **1**). Taking these components uniformly at random in [0, 1] to define two environments $\vec{\Lambda}^{(1)}$ and $\vec{\Lambda}^{(2)}$, we evolve two systems, one in each environment, and let them compete in the environment $\vec{\Lambda}^{(1)}$. The state resulting from this competition is very similar to the state of the system that evolved in the same environment ($s_{1,1+2}$ close to 1), and very dissimilar to the other state that evolved in a different environment ($s_{2,1+2}$ comparable to $s_{1,2}$). This is consistent with an adaptation of that system to its environment ($M = 10$, $T = 10^2$ as in Fig. 4).

the same "core" of reactions (12, 13), and stochastic transitions between states stem from fluctuations in the small numbers of molecules without requiring any additional "background" reactions. The mechanism that generates the different states is more akin to symmetry breaking, where a common set of constraints admits several different but related solutions (37).

Many chemical and physical models intended to imitate evolutionary dynamics are designed to alternate between phases of growth and fission, the latter typically triggered by external mechanical or thermal drives (3, 11, 38–40). This aims to achieve an overall exponential growth by enabling each separated product to regrow independently. While we could introduce advection to achieve a similar effect, we prefer to emphasize that exponential growth is not necessary to obtain the evolutionary properties that we describe, particularly exclusion by selection. Furthermore, a variant of our model with an appropriate spatial connectivity pattern through which diffusion occurs can exhibit exponential growth without alternation (*SI Appendix*, Fig. S8). Regarding exclusion, while exponential growth provides one mechanism through the competitive principle (41), it is not the only way, as illustrated in Fig. 2*A* and demonstrated in other contexts (14). Selection between states in our model also does not arise from competition for the supplied substrates $A_iA'_i$, which are never exhausted. Instead, selection arises from the relative stability of states and, when diffusion is limited, from an additional competition for space.

Our model relies on two fundamental properties of its building blocks: catalysis and specificity. We derive catalysis from fundamental physical principles, thus ensuring that it is a simple form of catalysis that can be implemented by rigid (inert) substances. Despite the inherent limitations of such simple catalysts, we demonstrate that any parameter values of the coarse-grained model are, in principle, achievable. Showing that the model can be realized without enzyme-like catalysts obviates the need to account for the emergence of such complex molecules. This contrasts, for example, with models with template replication of long heteropolymers mediated by polymerase-like catalysts, where the involvement of complex molecules to ensure accurate replication is thought to impose a constraint in the form of an error threshold (16). This also contrasts with models that require temperature cycles or other forms of external drives. Note that we could also make the catalyst C_i nonflowing, like minerals in some origin of life scenarios, and our results would not change. Specificity of the interactions is critical and requires a minimal form of complexity. Experimentally, this could be implemented with heteropolymers such as RNAs, which can form many specific interactions even with short sequences (42, 43). Other assumptions we have made, such as that all types are strictly equivalent, are for convenience and are not necessary.

Genericity is a key feature of our model. The basic dynamical mechanism requires a set of catalyzed reactions, in which the product of some reactions inhibits other reactions in a sparse and reciprocal manner. We have presented an implementation of this mechanism with the dissociation of dimers into monomers, but the reverse, binding reaction could be considered to achieve the same phenomenology. Autocatalytic reactions could also be considered, where there is no distinction between the catalyst and the product of the reactions, thus reducing the number of different elements. Beyond chemistry, the same principle drives multistability in models of ecological dynamics (18) and gene regulation (44). Indeed, the same mechanism of reciprocal inhibition is obtained in models where A_i represent individuals of a species born of other individuals of the same species, and inhibition takes the form of interspecies competition, or where they represent transcription factors transcribed by genes C_i, and inhibition takes the form of gene repression. In this latter context, a mechanism for biased jumps between two states has been proposed and demonstrated, where noise in gene expression allows for adaptive growth in the absence of explicit regulator (45). There, however, the bias stems from cellular growth and division, with no analogy to the mechanism of chemical growth by diffusion that our model exhibits. Above, we considered reciprocal inhibitory interactions, but the qualitative features are maintained even with some degree of asymmetry (18) (where the product of one reaction inhibits another reaction but not vice-verse). We also assumed stochasticity to arise from the small numbers of molecules but similar results could be obtained with large numbers of molecules if another source of stochasticity drives the transitions between states. Owing to the simple physical and generic mechanism on which it is based, our model can potentially be implemented in a variety of substrates at the molecular or colloidal level.

The model certainly lacks many characteristics associated with life, especially open-endedness (the potential for unlimited growth in complexity) and self-reference (no clear distinction between states and dynamical rules) (46): The state space is large but predefined and finite, and optimal productivity can be reached after a long but finite time. Evolution does not stop there, since further transitions occur between states, but not further adaptation. However, one can imagine generalizations in which, for example, a state in which both A_i and A_j are present in high concentration leads to the formation of substantial amount of a new dimer A_iA_j which can catalyze the formation of another A_k as C_k does, leading to a new state different from all those we have described, thus expanding the state space. This and other generalizations of the model are interesting directions for future work.

Data, Materials, and Software Availability. All study data are included in the article and/or *SI Appendix*.

ACKNOWLEDGMENTS. We are grateful to Philippe Nghe and Yann Sakref for their comments on an earlier draft.

1. J. Von Neumann *et al.*, *Theory of Self-Reproducing Automata* (University of Illinois press Urbana, 1966).
2. L. S. Penrose, Mechanics of self-reproduction. *Ann. Hum. Genet.* **23**, 59–72 (1958).
3. F. Zhou, R. Sha, H. Ni, N. Seeman, P. Chaikin, Mutations in artificial self-replicating tiles: A step toward Darwinian evolution. *Proc. Natl. Acad. Sci. U.S.A.* **118**, e2111193118 (2021).
4. G. v. Kiedrowski, A self-replicating hexadeoxynucleotide. *Angew. Chem. Int. Ed. Engl.* **25**, 932–935 (1986).
5. R. Schulman, B. Yurke, E. Winfree, Robust self-replication of combinatorial information via crystal growth and scission. *Proc. Natl. Acad. Sci. U.S.A.* **109**, 6405–6410 (2012).
6. A. I. Hanopolskyi, V. A. Smaliak, A. I. Novichkov, S. N. Semenov, Autocatalysis: Kinetics, mechanisms and design. *ChemSystemsChem* **3**, e2000026 (2021).
7. W. Hordijk, Autocatalytic confusion clarified. *J. Theor. Biol.* **435**, 22–28 (2017).
8. T. A. Lincoln, G. F. Joyce, Self-sustained replication of an RNA enzyme. *Science* **323**, 1229–1232 (2009).
9. M. Colomb-Delsuc, E. Mattia, J. W. Sadownik, S. Otto, Exponential self-replication enabled through a fibre elongation/breakage mechanism. *Nat. Commun.* **6**, 7427 (2015).
10. A. G. Cairns-Smith, The origin of life and the nature of the primitive gene. *J. Theor. Biol.* **10**, 53–88 (1966).
11. D. Segrè, D. Ben-Eli, D. Lancet, Compositional genomes: Prebiotic information transfer in mutually catalytic noncovalent assemblies. *Proc. Natl. Acad. Sci. U.S.A.* **97**, 4112–4117 (2000).
12. A. Blokhuis, D. Lacoste, P. Nghe, Universal motifs and the diversity of autocatalytic systems. *Proc. Natl. Acad. Sci. U.S.A.* **117**, 25230–25236 (2020).
13. V. Vasas, C. Fernando, M. Santos, S. Kauffman, E. Szathmáry, Evolution before genes. *Biol. Direct* **7**, 1 (2012).

14. Y. Sakref, O. Rivoire, On the exclusion of exponential autocatalysts by sub-exponential autocatalysts. *J. Theor. Biol.* **579**, 111714 (2023).
15. K. E. McGinness, G. F. Joyce, In search of an RNA replicase ribozyme. *Chem. Biol.* **10**, 5–14 (2003).
16. M. Eigen, Selforganization of matter and the evolution of biological macromolecules. *Naturwissenschaften* **58**, 465–523 (1971).
17. S. M. Marshall *et al*., Identifying molecules as biosignatures with assembly theory and mass spectrometry. *Nat. Commun.* **12**, 3033 (2021).
18. G. Bunin, Directionality and community-level selection. *Oikos* **130**, 489–500 (2021).
19. J. E. Ferrell, W. Xiong, Bistability in cell signaling: How to make continuous processes discontinuous, and reversible processes irreversible. *Chaos Interdiscip. J. Nonlinear Sci.* **11**, 227–236 (2001).
20. J. E. Ferrell, Tripping the switch fantastic: How a protein kinase cascade can convert graded inputs into switch-like outputs. *Trends Biochem. Sci.* **21**, 460–466 (1996).
21. O. Rivoire, Geometry and flexibility of optimal catalysts in a minimal elastic model. *J. Phys. Chem. B* **124**, 807–813 (2020).
22. M. Muñoz-Basagoiti, O. Rivoire, Z. Zeravcic, Computational design of a minimal catalyst using colloidal particles with programmable interactions. *Soft Matter* **19**, d3sm00194f (2023).
23. J. Barbier, F. Krzakala, L. Zdeborová, P. Zhang, The hard-core model on random graphs revisited. *J. Phys. Conf. Ser.* **473**, 012021 (2013).
24. Y. Fried, N. M. Shnerb, D. A. Kessler, Alternative steady states in ecological networks. *Phys. Rev. E* **96**, 012412 (2017).
25. C. H. Papadimitriou, K. Steiglitz, *Combinatorial Optimization: Algorithms and Complexity* (Courier Corporation, 1998).
26. W. Gardner *et al*., Self-organizing map and relational perspective mapping for the accurate visualization of high-dimensional hyperspectral data. *Anal. Chem.* **92**, 10450–10459 (2020).
27. F. Arceri, F. P. Landes, L. Berthier, G. Biroli, "Glasses and aging, a statistical mechanics perspective" in *Statistical and Nonlinear Physics*, B. Chakraborty, Ed. (Springer, New York, NY 2022), pp. 229–296.
28. C. Darwin, *On the Origin of Species by Means of Natural Selection, or the Preservation of Favoured Races in the Struggle for Life* (John Murray, London, 1859).
29. M. A. Nowak, H. Ohtsuki, Prevolutionary dynamics and the origin of evolution. *Proc. Natl. Acad. Sci. U.S.A.* **105**, 14924–14927 (2008).
30. E. Smith, H. J. Morowitz, *The Origin and Nature of Life on Earth: The Emergence of the Fourth Geosphere* (Cambridge University Press, 2016).
31. M. L. Wong *et al*., On the roles of function and selection in evolving systems. *Proc. Natl. Acad. Sci. U.S.A.* **120**, e2310223120 (2023).
32. T. Gánti, *The Principles of Life* (Gondolat, Budapest, 1971).
33. P. Decker, The origin of molecular asymmetry through the amplification of "stochastic information" (noise) in bioids, open systems which can exist in several steady states. *J. Mol. Evol.* **4**, 49–65 (1974).
34. J. Maynard Smith, E. Szathmáry, *The Major Transitions in Evolution* (Oxford University Press, Oxford, 1995).
35. M. Calvin, *Chemical Evolution: Molecular Evolution Towards the Origin of Living Systems on the Earth and Elsewhere* (Oxford: Clarendon P., 1969).
36. M. Calvin, Chemical evolution and the origin of life. *Am. Sci.* **44**, 248 (1956).
37. P. W. Anderson, D. Stein, "Broken symmetry, emergent properties, dissipative structures, life: Are they related?" in *Basic Notions Of Condensed Matter Physics* (CRC Press, 2018), pp. 263–277.
38. R. Schulman, E. Winfree, How crystals that sense and respond to their environments could evolve. *Nat. Comput.* **7**, 219–237 (2008).
39. X. He *et al*., Exponential growth and selection in self-replicating materials from DNA origami rafts. *Nat. Mater.* **16**, 993–997 (2017).
40. P. Adamski *et al*., From self-replication to replicator systems en route to de novo life. *Nat. Rev. Chem.* **4**, 386–403 (2020).
41. E. Szathmary, I. Gladkih, Sub-exponential growth and coexistence of non-enzymatically replicating templates. *J. Theor. Biol.* **138**, 55 (1989).
42. J. SantaLucia Jr., A unified view of polymer, dumbbell, and oligonucleotide DNA nearest-neighbor thermodynamics. *Proc. Natl. Acad. Sci. U.S.A.* **95**, 1460–1465 (1998).
43. D. Semizarov *et al*., Specificity of short interfering RNA determined through gene expression signatures. *Proc. Natl. Acad. Sci. U.S.A.* **100**, 6347–6352 (2003).
44. T. S. Gardner, C. R. Cantor, J. J. Collins, Construction of a genetic toggle switch in *Escherichia coli*. *Nature* **403**, 339–342 (2000).
45. C. Furusawa, K. Kaneko, A generic mechanism for adaptive growth rate regulation. *PLoS Comput. Biol.* **4**, e3 (2008).
46. N. Goldenfeld, C. Woese, Life is physics: Evolution as a collective phenomenon far from equilibrium. *Annu. Rev. Condens. Matter Phys.* **2**, 375–399 (2011).